JURNAL UPI

Indonesian Journal of Science & Technology

Journal homepage: http://ejournal.upi.edu/index.php/ijost/

IJoST Indonesian Journal of Science & Technology

Working Volume and Milling Time on the Product Size/Morphology, Product Yield, and Electricity Consumption in the Ball-Milling Process of Organic Material

Asep Bayu Dani Nandiyanto [1], Riezqa Andika [2], Muhammad Aziz [3], Lala Septem Riza [4]*

[1]Departemen Kimia, Universitas Pendidikan Indonesia, Jl. Dr. Setiabudi no 229, Bandung 40154, Indonesia
[2]School of Chemical Engineering, Yeungnam University, Gyeongsan, South Korea
[3]Institute of Innovative Research, Tokyo Institute of Technology, 2-12-1 Ookayama, Meguro-ku, Tokyo, Japan
[4]Departemen Teknik Informatika, Universitas Pendidikan Indonesia, Jl. Dr. Setiabudi no 229, Bandung 40154, Indonesia.
*Corresponding author: Email: nandiyanto@upi.edu; Tel/fax: +62 22 200 0579

ABSTRACT

Analysis of ball-milling process under various conditions (i.e. working volume, milling time, and material load) on the material properties (i.e. chemical composition, as well as particle size and morphology), product yield, and electricity consumption was investigated. Turmeric (*curcuma longa*) was used as a model of size-reduced organic material due to its thermally and chemically stability, and fragile. Thus, clear examination on the size-reduction phenomenon during the milling process can be done without considering any reaction as well as time-consuming process. Results showed that working volume is prospective to control the characteristics of product. Working volume manages the shear stress and the collision phenomena during the process. Specifically, the lower working volume led to the production of particles with blunt-edged morphology and sizes of several micrometers. Although working volume is potentially used for managing the final particle size, this parameter has a direct impact to the product yield and electricity consumption. Adjustment of the milling time is also important due to its relation to breaking material and electrical consumption.

ARTICLE INFO

Article History:
Submitted/ Received 01 May 2018
First Revised 05 Jun 2018
Accepted 20 Aug 2018
First available online 28 Aug 2018
Publication Date 01 Sep 2018

Keywords:
Ball-milling process,
collision,
economic evaluation,
curcumin,
working volume.

DOI: http://dx.doi.org/10.17509/ijost.v3i2.12752 |
p- ISSN 2528-1410 e- ISSN 2527-8045 |

1. INTRODUCTION

High-energy ball-milling process has attracted tremendous attention for decades since this process is effective for reducing material size (Islam *et al.*, 2013; Koch, 2003; Stolle *et al.,* 2011). This process has been well-applied in practical uses for various materials (Stolle et al., 2011). This process has been also combined with other types of processes (Bazazi *et al.,* 2018; Dai *et al.,* 2018; Dalmis *et al.,* 2018; Kutuk & Kutuk-Sert, 2017; Lv *et al.,* 2014).

In a short version of the procedure, the material and balls are loaded into a milling vial. The milling vial is then rotated to create interaction of balls against each other and the vial's wall. Indeed, when the material is located in between interacting balls, the material gets broken (Nandiyanto *et al.,* in press-b).

To get optimum condition in reducing the final particle size, many parameters must be considered (Stolle *et al.,* 2011), such as the milling time (Li *et al.,* 2018; Lv *et al.,* 2014; Wang *et al.,* 2018), the milling speed (Gao & Forssberg, 1993; Li *et al.,* 2018; Mio *et al.,* 2002; Zhang *et al.,* 2008), the milling temperature (Gaffet, 1991), the ball and material load (Li *et al.,* 2018; Zhang *et al.,* 2008), the sizes of ball and material (Zhang *et al.,* 2008), the physicochemical properties of ball and material (Gao & Forssberg, 1993), the volume of reactor (Zhang et al., 2008), the milling vial diameter, the working volume (Nandiyanto *et al.,* in press-b), and the contact time between ball and material as well as the collision energy (Nandiyanto *et al.,* in press-b). Among the aforementioned parameters, working volume is one of the most attractive parameters since it has direct correlations to the amount of input/output in the ball-milling process (Nandiyanto *et al.,* in press-b) and the control of the final product characteristics (Mishra & Rajamani, 1992). Indeed, this will relate to the scaling process. However, current studies described successful size-reduction process with only partial information on product performance, electricity consumption, and product yield in the ball-milling process. In fact, this information is important to be added as a contributive factor for understanding the implementation of ball-milling process in the realistic condition.

In our previous studies (A. B. Nandiyanto *et al.,* 2017; Nandiyanto *et al.,* in press-b), we have investigated the ball-milling process for preparing carbon materials. In short, we have confirmed that controlling parameters have a great impact to the breakage characteristics of the size-reduced material. However, our previous studies have limitations to unconcern of the type of size-destructed materials as well as economic assessment of the ball-milling process (i.e. product yield and electricity consumption).

Considering the rationale, the purpose of this study was to evaluate the influences of working volume and milling time on the characteristics of products and the economic assessment (i.e. product yield and electricity usage) of the ball-milling process. As a model of size-destructed organic material, turmeric (curcuma longa) was used. Different from other organic materials that are typically reactive, turmeric is relatively chemically and thermally inert. Indeed, since the ball-milling process relates to the collision that can lead the chemical reaction (Stolle *et al.,* 2011; Suryanarayana, 2001), the use of turmeric is effective and appropriate for examining phenomenon happening during the milling process without considering any chemical reaction. Furthermore, dried turmeric is fragile and brittle, making that the turmeric is easily destroyed and the ball-milling does not correlate with the time-consuming process. To get the evaluation precisely, milling condition was varied: milling time (from 0 to 40 minutes) and working volume (from 0 to 100% of the working volume). During the variation of milling condition, other milling

DOI: http://dx.doi.org/10.17509/ijost.v3i2.12752 |
p- ISSN 2528-1410 e- ISSN 2527-8045 |

parameters (i.e. milling speed/rotation, ball-to-component ratio, milling temperature, and ball size) were kept constant. The process was done in the batch-typed conventional ball-milling process. This type of ball-milling process was selected as a model because of two reasons (Nandiyanto *et al.,* in press-b): (i) minimizing air circulation amount that can affect the oxidation. This can be done since there is no access for material and heat to go in/out the system; and (ii) creating the gravitational force as the main size-reduction parameter in the milling process. Indeed, other influencing parameters can be neglected and the analysis can be focused on the specific parameters, i.e. milling time and working volume.

In addition, to make readers understand the main reason for the importance of working volume, the analysis was completed with theoretical approximation and analysis. The evaluation of the product yield and electricity consumption under various working volumes was also presented since it can be a contributive factor to determine the optimum condition of the ball-milling process.

2. EXPERIMENTAL METHOD

The experimental procedure involves: (i) specimen preparation (including slicing, drying, and saw-milling processes) and (ii) ball-milling process. **Figure 1** is added to clarify the experiment procedure conducted in this study.

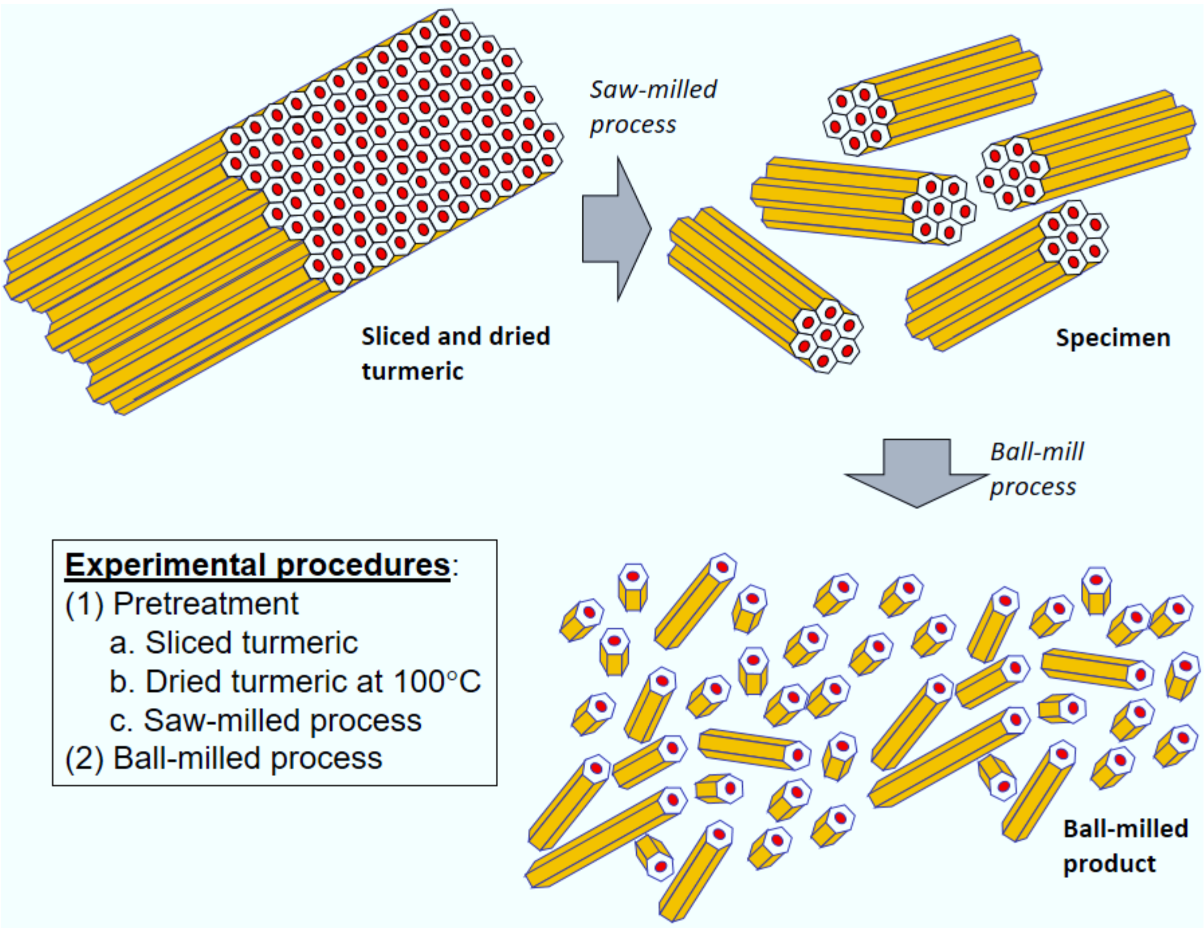

Figure 1. Experimental procedures.

DOI: http://dx.doi.org/10.17509/ijost.v3i2.12752 |
p- ISSN 2528-1410 e- ISSN 2527-8045 |

2.1. Specimen preparation

Turmeric (*curcuma longa*; obtained from Bandung, Indonesia) was washed, dried, and sliced into small pieces (sizes of about 5 mm). The sliced turmeric was then re-dried at 50°C for 10 hours (for removing physically adsorbed water on the surface of the sliced turmeric). Subsequently, the turmeric was heated at temperature of 100°C for 4 hours (for removing major water content in the turmeric). Detailed information for the preparation of dried turmeric is shown in our previous reports (Nandiyanto *et al.,* 2017; Nandiyanto *et al.,* 2017; Nandiyanto *et al.,* 2018; Nandiyanto *et al.,* 2016; Nandiyanto *et al.,* in press-a).

The dried turmeric was then put into a batch-typed saw-milling apparatus. The present saw-milling apparatus is a cylinder milling vial (polytetrafluoroethylene; diameter = 7 cm; height = 10 cm) equipped with a single stainless steel blade unit (attached in the center bottom of the vial). The blade unit has four jigsaw blades: two blades are horizontal and the other two are upwards in about 45 degrees. Each blade has dimension of 3 cm in length. The saw-milling process was conducted at 18,000 rpm for 5 minutes followed by manual mixing (using a metal spoon). To get a homogenous milling process, the combination of milling and manual mixing was done five times. The prepared powder is named as the specimen.

2.2. Ball-milling process

Prior to the ball-milling process, the specimen was pretreated at 70°C for 1 hour to remove physically adsorbed water on the surface of the specimen. The pretreated specimen was then put into a batch-typed conventional type ball-milling apparatus. In general, the ball-milling apparatus itself consists of cylinder milling vial (stainless steel; diameter = 14 cm; length = 7 cm) and 8-mm stainless steel balls. The ball-milling process was conducted at room temperature, a milling vial rotation speed of 100 rpm, and the mass ratio of ball and specimen of 100. In this study, the milling time varied from 0 to 60 minutes, and the working volume was varied from 0 to 100%. In addition, to obtain the product yield, the mass of the product was compared to the initial mass of specimen.

2.3. Characterization

Several characterizations were performed: Scanning electron microscope (SEM; JSM-6360LA; JEOL Ltd., Japan; to analyze the morphology and size of the product, Fourier transform infra red (FTIR, FTIR-6600, Jasco Corp., Japan; to analyze the elemental structure of the product); Thermal Gravimetry Analysis and Differential Thermal Analysis (TGA-DTA; Shimadzu Corp., Japan; to analyze the thermal behaviour of the turmeric). To analyze the electricity usage under various working volume and milling time, the ball-milling apparatus was connected to the commercially available power wattmeter. In addition, to get precise size analysis based on the SEM images, a measurement using Ferret analysis of more than 100 individual particles was used.

3. RESULTS AND DISCUSSION

3.1. Physicochemical properties of the turmeric as the model for size-destruction organic material.

Figure 2 shows the TG analysis results of the specimen. The mass degradation begins from 60°C and ends at about 500°C. Gradual decreases in mass was found in several steps, and the steps are shown in vertical dashed line. The mass after 100°C was more than 95%, whereas the final mass after 500°C is 20%. The final mass was obtained as a black powder, informing that specimen has completely decomposed into carbon. This indicates that the additional heat affects to the change of physicochemical properties of turmeric.

DOI: http://dx.doi.org/10.17509/ijost.v3i2.12752 |
p- ISSN 2528-1410 e- ISSN 2527-8045 |

Different from other reports regarding the thermal characteristics of curcumin that typically contain two stages (Chen *et al.,* 2014), the thermal characteristic of turmeric has seven stages. The difference in the thermal decomposition stage is because of the existence of complex chemical composition and structures inside the turmeric that is different from pure curcumin. At least, turmeric contained three main compounds: curcumin, demethoxycurcumin, and bisdemethoxycurcumin. Turmeric also constitutes 50–60% of the curcuminoids, while the other components are essential oils such as monocyclic monoterpenes, sesqui terpene (bisabolanes and germacranes), arabinogalactans, and ar-turmerone (Mishra, 2009). The confluence of these components makes the turmeric stable at temperature of less than 150°C (Nandiyanto *et al.,* 2017). Indeed, this is verified by the TG mass loss of less than 5% at between 60 and 100°C (see **Figure 2**), in which this mass loss is from the release of the physically adsorbed water in the sample. This result describes why the pretreatment process by heating at temperature of less than 100°C prior to the ball-milling process must be done.

As discussed above in the thermal characteristic analysis, the turmeric is relatively chemically and thermally stable in the range of less than 150°C. Since the changes in the temperature during the ball-milling process are not so high (Koch, 2003), the TG analysis confirmed that turmeric is prospective to be used as a model of size-destructed organic material.

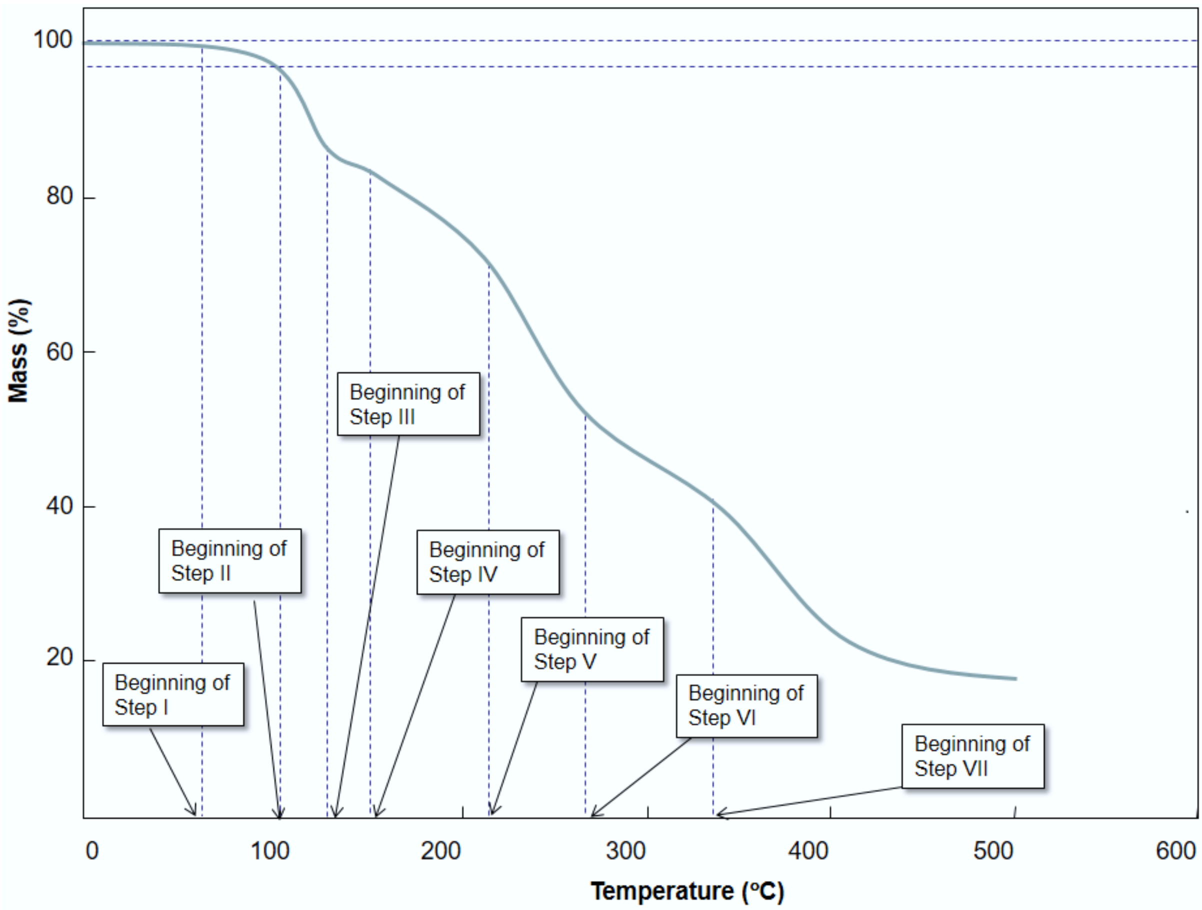

Figure 2. TG analysis of specimen.

DOI: http://dx.doi.org/10.17509/ijost.v3i2.12752 |
p- ISSN 2528-1410 e- ISSN 2527-8045 |

3.2. Effect of milling time in the ball-milling process

Figure 3a shows the size distribution analysis result under various milling times using working volume of 30%. This result showed that the initial particles (after saw-milling process) have broad size distribution. Then, the maximum peak of the size distribution shifted to a smaller size as processing time extended. The optimum milling time was obtained when applying 30 minutes of the milling process. The longer milling time seemed to have no more impact to the size-reduction process.

Figure 3b presents the analysis of the total electricity used in the milling process. Various working volumes were evaluated. The result showed similar trends in the electricity consumption. The longer milling time has a direct correlation to the more total electricity consumption must be employed. The results also showed that the more working volume give consequence in the more efficient in the electricity usage, and further the cost of the production. Compared to **Figure 3a**, the results conclude that the optimum milling time is 30 minutes with the working volume of more than 30%. Applying longer milling time has increase the cost but has no great impact to reduce the particle size.

3.3. Effect of milling time in the ball-milling process

Figure 4 shows the chemical analysis results of the specimen using FTIR. Identical patterns for all samples (before and after the milling process) were detected. The difference was obtained only in peak intensities (see the vertical dashed line).

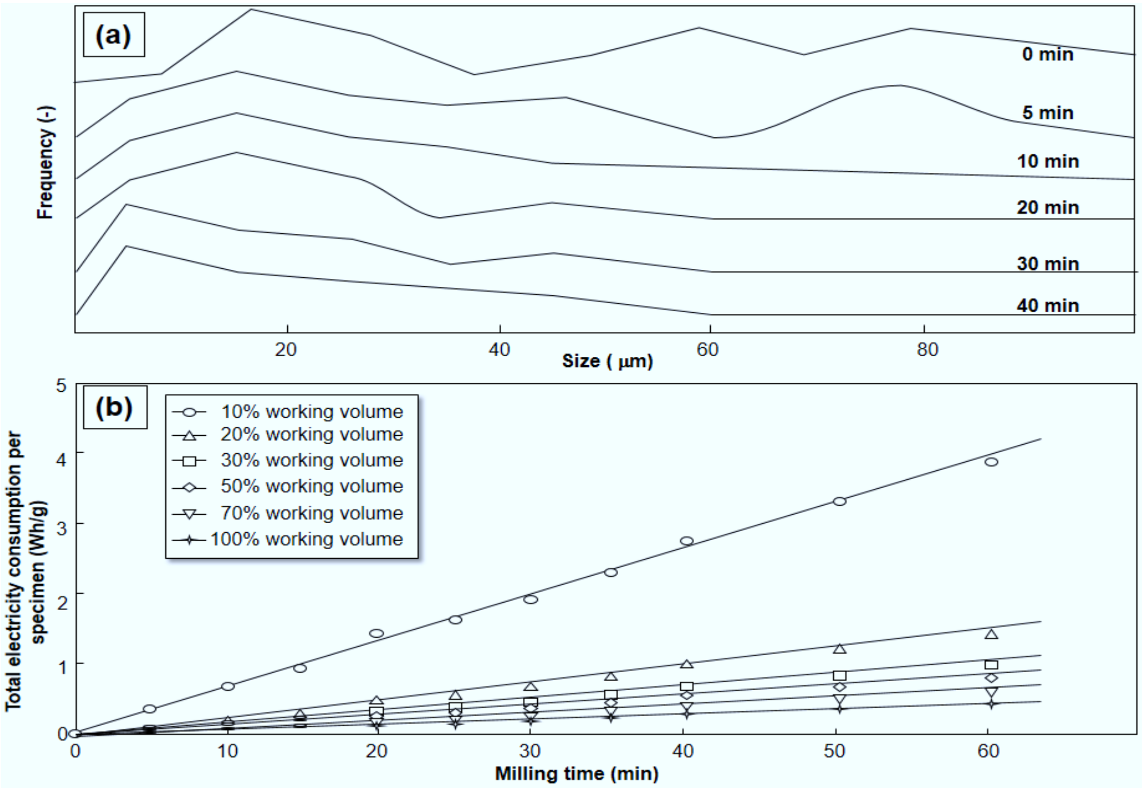

Figure 3. Analysis result of the size distribution (a) and the total electricity used per specimen (b) in the ball-milling process as a function of milling time.

DOI: http://dx.doi.org/10.17509/ijost.v3i2.12752 |
p- ISSN 2528-1410 e- ISSN 2527-8045 |

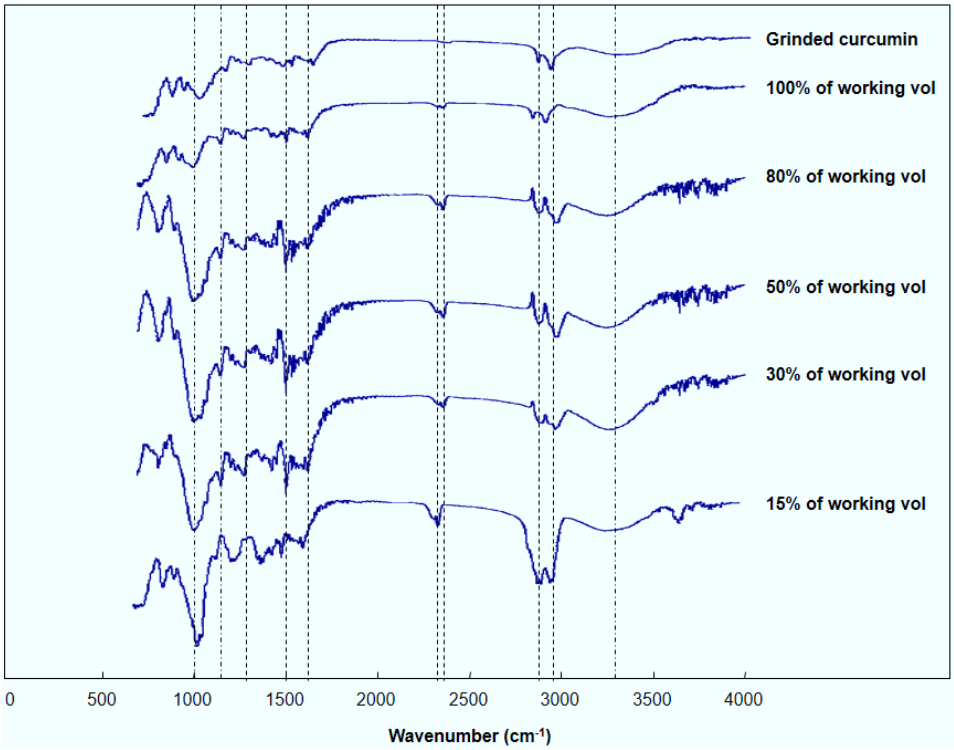

Figure 4. The FTIR analysis results of specimens prepared with various working volumes.

Tabel 1. Functional group obtained from FTIR analysis. Data was compared with reference (Nandiyanto *et al.,* 2017)

Wavenumber (cm^{-1})		Assignment
Experiment	Literature	
3350	3510	Phenolic O–H stretching
1515	1627	C=C vibrations
1635	1656	C-O stretch
1400	1427	Olefinic C–H bending vibration
1165	1285	Aromatic C–O stretching vibrations
1019	840	C–O–C stretching vibrations
	1027	
2976	2845	C-H methyl ring
2932	3016	Aromatic ring

To confirm the analysis of the FTIR peaks, **Table 1** shows the comparison results between the present FTIR peaks and the literature (Nandiyanto *et al.,* 2017; Nandiyanto *et al.,* 2017). The analysis showed that all specimens had specific spectra of curcuminod material, such as about 1400 (olefinic C–H bending vibration), 1500 (C=C vibrations), as well as 1600 cm^{-1} (C-O stretch).

Prior to discussing the phenomena happening during the ball-milling process, FTIR analysis of the specimen with various ball-milling process was conducted (See **Figure 4**). The FTIR detected that all samples had similar

DOI: http://dx.doi.org/10.17509/ijost.v3i2.12752 |
p- ISSN 2528-1410 e- ISSN 2527-8045 |

peaks and patterns for the dried turmeric, specimen, and specimen after ball-milling process. Although there is a difference, changes were identified only in the FTIR intensities. Lower working volume results in the higher FTIR peak intensities. The main reason is because lower working volume has correlations to the more air content in the reactor vial. Indeed, this can give consequences to the oxidation process. However, since the milling process is a sealed system, the air circulation as well as the oxidation process can be minimized (Nandiyanto *et al.,* in press-b).

The changes in the FTIR peak intensity at about 3200 cm^{-1} related to the change in the OH-related material. The smaller powder has correlations to the larger surface area. Indeed, since turmeric can absorb water, larger surface area relates to the more water contained in the sample (the water can be from air and oxidation process).

Other possibilities for the hypothesis in the change of intensity at about 2400 cm^{-1} and the curcuminoid specific peaks are due to the reduction of the particle size. Since curcumin in the turmeric specimen forms as a polymeric structure, the reduction of size has a correlation to the breakage of the polymer. With the creation of smaller molecules, it results in the identification of higher curcuminoid peak intensities.

Figure 5 depicts the SEM analysis images of the specimen. Differences in shape and size for specimen before and after the milling process were obtained.

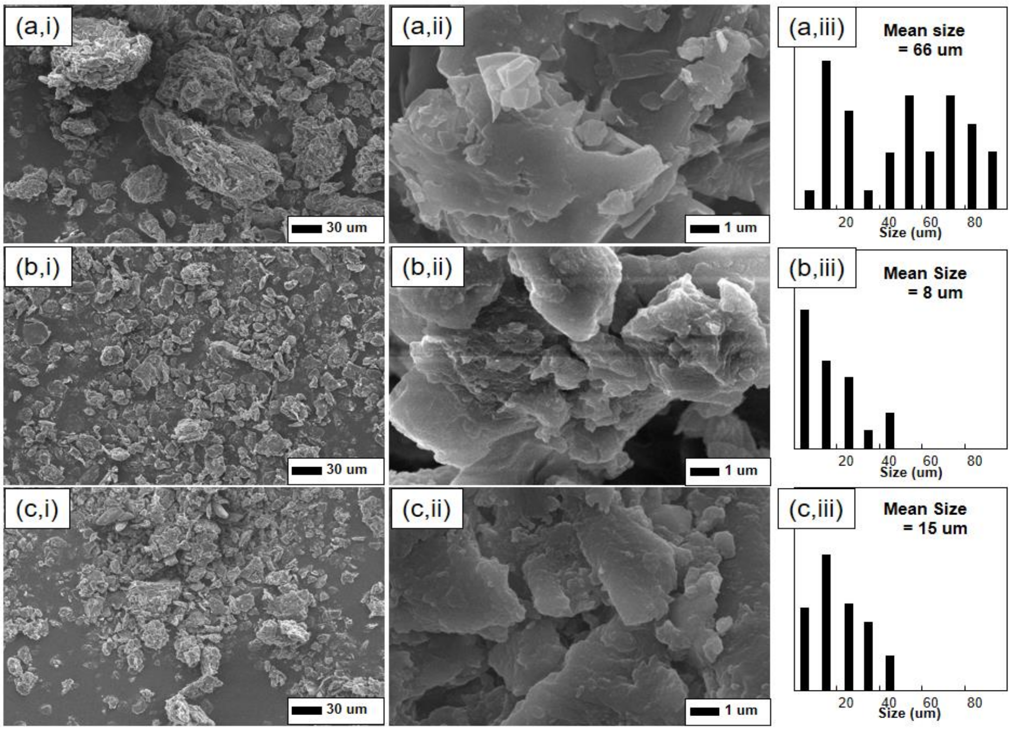

Figure 5. The SEM analysis images of specimen under various working volumes: (a) specimen (before ball-milling process), (b) 70, and (c) 30%. Figures (a,i), (b,i), and (c,i) are the results of low-magnified SEM image. Figures (a,ii), (b,ii), and (c,ii) are the results of high-magnified SEM image. Figures (a,iii), (b,iii), and (c,iii) are the Ferret analysis results.

DOI: http://dx.doi.org/10.17509/ijost.v3i2.12752 |
p- ISSN 2528-1410 e- ISSN 2527-8045 |

The sliced turmeric before and after the saw-milling process have identical shape with a size dimension of about 5,000 μm (not displayed). Slight change in size and shape was found, in which this is due to the removal of water content from the turmeric.

Applying the saw-milling process to the dried turmeric results in the formation of particles with smaller sizes (sizes of about 66 μm) (Figure 5(a,i)). The reduction in the size from their originated dried turmeric was obtained, confirming that the saw-milling process is effective for the size-reduction process. However, the size reduction has limitations to sizes of down to dozens micrometers.

The additional ball-milling process to the saw-milled samples led to the more size-reduction process (**Figures 5**(**b**,**i**) and (**c**,**i**)). As shown in **Figure 5**(**b**,**i**), the particle size decreased to the mean size of 15 micrometers when using working volume of 70%. Further decreases were found when using lower working volume, which allow to the production of particles with sizes of several micrometers (**Figure 5**(**c**,i)).

To confirm the morphology of the particles, high magnification of SEM images are presented in **Figures 5**(**a**,**ii**), (**b**,**ii**), and (**c**,**ii**). Interesting results were obtained. The saw-milled products have sharp edge and some of them are needle shapes (**Figure 5**(**a**,**ii**)). The ball-milled products have blunt edge (**Figures 5**(**b**,**ii)** and (**c**,**ii**)). Different from the saw-milling process, the ball-milling process allows to the production of submicrometer-sized particles.

The size distribution of products is presented in **Figures 5**(**a**,**iii**), (**b**,**iii**), and (**c**,**iii**). The results replied that the working volume has impact to the change in the final particle size distribution. Particles with a broad size distribution were obtained when using 100% of working volume. Then, when using lower working volume, the smaller particles with narrower size distribution were produced.

As shown in **Figure 5**, the saw-milling process is potentially used for reducing particle size down to dozens micrometers, whereas the ball-milling process is prospective to produce particles with sizes of down to submicrometers. The main idea for the effectiveness of the ball milling compared to saw-milling in reducing particle size is due to the type of destruction. However, nanometer-sized particles cannot be produced. Indeed, to reduce particle sizes of down to nanometer-ranged particles, additional techniques must be added (Nandiyanto *et al.,* in press-b).

Differences in particle shape and size were obtained when varying working volumes (see **Figure 5**). The existence of shear stress and collisions among balls during the ball-milling process is the main reason.

In short, the process with full working volume will give shear stress only during the size-reduction phenomena. Since the shear stress seems to have lower impact on destroying material (Nandiyanto *et al.,* in press-b), incomplete size destruction occurs. Indeed, the final product has still contained larger particles. On the contrary, process with lower working volume relates to the availability of free air space in the milling vial. This promotes the components (i.e. balls and turmeric specimens) inside the vial to move easily as well as to do cataracting and fracturing condition (Burmeister & Kwade, 2013). Indeed, this leads to more collision phenomena in addition to the shear stress (Nandiyanto *et al.,* in press-b). As a consequence, smaller particles were obtained in the final product.

Correlation between working volume and mean particle size as well as product yield and electricity usage is shown in **Figure 6**. The working volumes of 100, 70, 50, 30, and 20% allow to the reduction of particle mean sizes to about 66, 15, 10, 9, and 8 μm, respectively.

DOI: http://dx.doi.org/10.17509/ijost.v3i2.12752 |
p- ISSN 2528-1410 e- ISSN 2527-8045 |

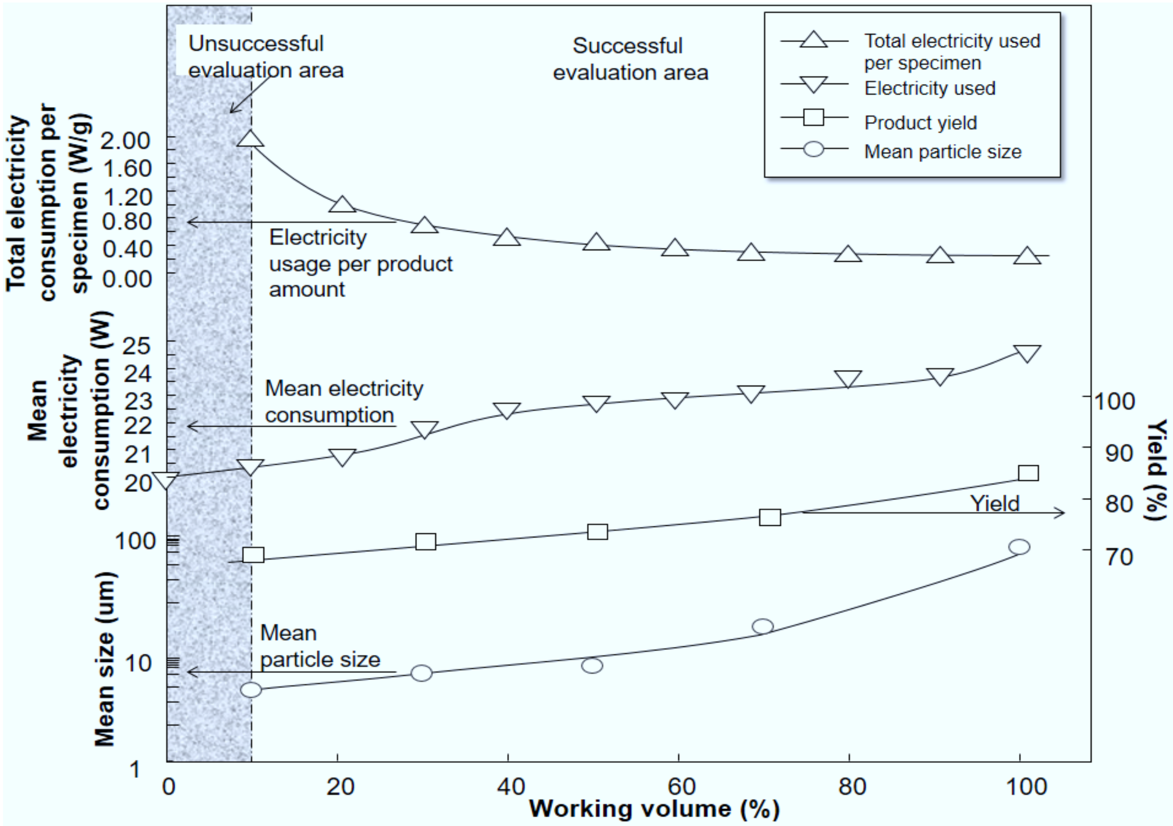

Figure 6. Correlation of working volume with mean size, product yield, electricity required in the ball-milling process

In addition to the influence of working volume on the particle size, analysis of the product yield was evaluated. The larger working volume is used, the higher product yield is obtained.

Regarding the electricity consumption in the ball-milling process, the larger working volume resulted in the higher electricity cost required. However, consideration of the electricity only cannot be used to determine techno-economic assessment. Thus, ratio between electricity and specimen mass must be done. The correlation showed that the lower working volume has higher the ratio of electricity cost and specimen amount. However, when the working volume is larger than 40%, the value of the ratio seemed to be similar (near to 0.40 Wh/g).

Based on **Figure 6**, although less working volume is prospective for creating particles in the range of several micrometers, there is a problem that must be faced regarding the product yield and electricity consumption efficiency. The less working volume there is, the fewer product yields can be obtained. The possibility of some products to be attached on the balls and vial is the main reason (Nandiyanto *et al.,* in press-b). Even though the process uses different working volume, the number of attached products tends to be equal. The process with lower working volume will have lower ratio between final and attached products than that with higher working volume.

In addition to the product yield, the analysis of the electricity consumption must be added. The more working volume has correlation to the higher electricity consumption for the milling production (as shown in **Figure 6**). Working volume correlates with the material and ball load. Indeed, when using the more working volume, the more load must be moved inside the apparatus, creating the more energy required.

Consideration of the electricity consumption only cannot be used to determine the techno-economic assessment of ball-milling process. Analysis must be compared with the amount of specimen being size-reduced. The correlation in **Figure 6** showed that the lower working volume has higher the ratio of electricity cost and specimen amount. However, since the working volume of larger than 40% has identical value of the ratio between electricity consumption and specimen amount (near to 0.40 Wh/g). This result showed that optimization of the working volume must be done to get efficient production.

Based on the above correlations, the optimum condition to get submicrometer-sized particles with narrow size distribution must be done in the working volume of between 30 and 50% and milling time of 30 minutes. Deviation from this value will create inefficient techno-economic assessment (i.e. product yield and electricity consumption-to-specimen amount ratio.

4. CONCLUSION

Influences of ball-milling process condition (i.e. working volume, milling time, and material load) on the material characteristics (including particle size and morphology, as well as chemical composition) and economic assessment (i.e. product yield and electricity consumption) have been investigated. Experimental results confirmed the effectiveness of working volume as a main parameter for the control the breakage characteristics of materials. The working volume manages the existence of shear stress and collision phenomena during the ball-milling process. The lower working volume results in the production of smaller particles with blunt-edged morphology. Although working volume is potentially used for controlling the particle size, this parameter has a direct impact to the product yield and electricity used. Thus, optimization of the process condition is highly required, especially in regard to practical uses, scaling up production, and other development of ball-milling process.

5. ACKNOWLEDGEMENTS

RISTEK DIKTI (Grant-in-aid Penelitian Terapan Unggulan Perguruan Tinggi (PTUPT) and Penelitian Unggulan Strategi Nasional (PUSN)) is acknowledged.

6. AUTHORS' NOTE

The author(s) declare(s) that there is no conflict of interest regarding the publication of this article. Authors confirmed that the data and the paper are free of plagiarism..

7. REFERENCES

Bazazi, S., Arsalani, N., Khataee, A., & Tabrizi, A. G. (2018). Comparison of ball milling-hydrothermal and hydrothermal methods for synthesis of ZnO nanostructures and evaluation of their photocatalytic performance. *Journal of industrial and engineering chemistry, 62*, 265-272.

Burmeister, C. F., & Kwade, A. (2013). Process engineering with planetary ball mills. *Chemical Society Reviews, 42*(18), 7660-7667.

Chen, Z., Xia, Y., Liao, S., Huang, Y., Li, Y., He, Y., Tong, Z., & Li, B. (2014). Thermal degradation kinetics study of curcumin with nonlinear methods. *Food chemistry, 155*, 81-86.

Dai, L., Li, C., Zhang, J., & Cheng, F. (2018). Preparation and characterization of starch nanocrystals combining ball milling with acid hydrolysis. *Carbohydrate polymers, 180*, 122-127.

Dalmis, R., Cuvalci, H., Canakci, A., Guler, O., & Celik, E. (2018). The Effect of Mechanical Milling on Graphite–Boron Carbide Hybrid Reinforced ZA27 Nanocomposites. *Arabian Journal for Science and Engineering, 43*(3), 1113-1124.

Gaffet, E. (1991). Planetary ball-milling: an experimental parameter phase diagram. *Materials Science and Engineering: A, 132*, 181-193.

Gao, M.-W., & Forssberg, E. (1993). A study on the effect of parameters in stirred ball milling. *International Journal of Mineral Processing, 37*(1-2), 45-59.

Islam, S., Al-Eshaikh, M., & Huda, Z. (2013). Synthesis and characterization of high-energy ball-milled tungsten heavy alloy powders. *Arabian Journal for Science and Engineering, 38*(9), 2503-2507.

Koch, C. (2003). Top-down synthesis of nanostructured materials: Mechanical and thermal processing methods. *Reviews on Advanced Materials Science, 5*(2), 91-99.

Kutuk, S., & Kutuk-Sert, T. (2017). Effect of PCA on nanosized ulexite material prepared by mechanical milling. *Arabian Journal for Science and Engineering, 42*(11), 4801-4809.

Li, X., Kokawa, M., & Kitamura, Y. (2018). Influence of micro wet milling parameters on the processing of Komatsuna (Brassica rapa var. perviridis) juice with rich phosphatidic acid. *Journal of Food Engineering, 217*, 50-57.

Lv, Y.-J., Su, J., Long, Y.-F., Lv, X.-Y., & Wen, Y.-X. (2014). Effect of milling time on the performance of bowl-like LiFePO 4/C prepared by wet milling-assisted spray drying. *Ionics, 20*(4), 471-478.

Mio, H., Kano, J., Saito, F., & Kaneko, K. (2002). Effects of rotational direction and rotation-to-revolution speed ratio in planetary ball milling. *Materials Science and Engineering: A, 332*(1-2), 75-80.

Mishra, B., & Rajamani, R. K. (1992). The discrete element method for the simulation of ball mills. *Applied Mathematical Modelling, 16*(11), 598-604.

Mishra, P. (2009). Isolation, spectroscopic characterization and molecular modeling studies of mixture of Curcuma longa, ginger and seeds of fenugreek. *International Journal of PharmTech Research, 1*(1), 79-95.

Nandiyanto, A., Wiryani, A., Rusli, A., Purnamasari, A., Abdullah, A., & Riza, L. (2017). Decomposition Behavior of Curcumin during Solar Irradiation when Contact with Inorganic Particles. *IOP Conference Series: Materials Science and Engineering, 180*, 012135.

Nandiyanto, A., Wiryani, A., Rusli, A., Purnamasari, A., Abdullah, A., Widiaty, I., & Hurriyati, R. (2017). Extraction of Curcumin Pigment from Indonesian Local Turmeric with Its Infrared Spectra and Thermal Decomposition Properties. *IOP Conference Series: Materials Science and Engineering, 180*, 012136.

Nandiyanto, A., Zaen, R., Oktiani, R., & Abdullah, A. (2018). Photodecomposition Profile of Curcumin in the Existence of Tungsten Trioxide Particles. *IOP Conference Series: Materials Science and Engineering, 306*, 012002.

Nandiyanto, A. B., Putra, Z. A., Andika, R., Bilad, M. R., Kurniawan, T., Zulhijah, R., & Hamidah, I. (2017). Porous activated carbon particles from rice straw waste and their adsorption properties. *Journal of Engineering Science and Technology, 12*, 1-11.

Nandiyanto, A. B. D., Sofiani, D., Permatasari, N., Sucahya, T. N., Wiryani, A. S., Purnamasari, A., Rusli, A., & Prima, E. C. (2016). Photodecomposition profile of organic material during the partial solar eclipse of 9 march 2016 and its correlation with organic material concentration and photocatalyst amount. *Indonesian Journal of Science and Technology, 1*(2), 132-155.

Nandiyanto, A. B. D., Zaen, R., & Oktiani, R. (in press-a). Correlation between crystallite size and photocatalytic performance of micrometer-sized monoclinic WO3 particles. *Arabian Journal of Chemistry*.

Nandiyanto, A. B. D., Zaen, R., & Oktiani, R. (in press-b). Working Volume in High-Energy Ball-Milling Process on Breakage Characteristics and Adsorption Performance of Rice Straw Ash. *Arabian Journal for Science and Engineering*.

Stolle, A., Szuppa, T., Leonhardt, S. E., & Ondruschka, B. (2011). Ball milling in organic synthesis: solutions and challenges. *Chemical Society Reviews, 40*(5), 2317-2329.

Suryanarayana, C. (2001). Mechanical alloying and milling. *Progress in materials science, 46*(1-2), 1-184.

Wang, B., Wei, S., Wang, Y., Liang, Y., Guo, L., Xue, J., Pan, F., Tang, A., Chen, X., & Xu, B. (2018). Effect of milling time on microstructure and properties of Nano-titanium polymer by high-energy ball milling. *Applied Surface Science, 434*, 1248-1256.

Zhang, F., Zhu, M., & Wang, C. (2008). Parameters optimization in the planetary ball milling of nanostructured tungsten carbide/cobalt powder. *International Journal of Refractory Metals and Hard Materials, 26*(4), 329-333.